Instability analysis in incremental rotary forming of tube flanges

Bhaskaran Krishnamurthy[a]*, Olga Bylya[a], Kyle Watt[a], Alastair Conway[a], Martin Tuffs[c], Paul Blackwell[b]

[a] Advanced Forming Research Centre, University of Strathclyde, 85 Inchinnan Drive, Inchinnan – PA49LJ, United Kingdom
[b] Design, Manufacture & Engineering Management | University of Strathclyde, James Weir Building, 75 Montrose St, Glasgow - G1 1XJ, United Kingdom
[c] Rolls-Royce plc, PO Box 31, Derby, DE24 8BJ

*Corresponding author: bhaskaran.krishnamurthy@strath.ac.uk

Abstract
Rotary forming is an exciting route for forming flanges of different angles from seamless tubes of high-strength materials. True to its incremental nature, the process offers great flexibility, but the issues encountered are atypical and complex. One such issue observed in experimental trials is the internal buckling of tubes during specific instances of flange formation. The origin of this instability is non-trivial, and ordinarily, finite-element (FE) models fail to capture this instability. To analyse and understand the problem, systematic experimental trials were carried out using different tube thicknesses, tube materials and tool kinematics. This paper summarises the results from a critical analysis to establish (1) a criteria for quantifying the instability and identifying the instances of its occurrence, (2) a validation methodology to fine-tune FE models for the process, and (3) use of FE models to understand the influence of tool path in the flange forming stage.

Keywords: Rotary Forming, Flange forming, Incremental bulk forming, Process instabilities, Tool kinematics

1. Introduction
Rotary forming is an incremental bulk forming process that affords the possibility to form a wide range of tubular components using simple sets of tools prescribing a complex tool path [(Groche et al. 2007), (Tamang et al. 2017)]. The high degrees of freedom (DoF) and highly localised area of deformation makes it a very flexible process. For instance, the components shown in Figure 1(a) were all made from a simple conical top tool and a hollow cylindrical bottom tool (shown in Figure 1(b,c)). By forming the flanges from a seamless tube, there is a significant reduction in material wastage as opposed to traditional machining operations; and by using incremental loading it is possible to produce very high deformations (50-100%) in high-strength materials with limited ductility (12%) at room temperature using a small machine, as opposed to traditional flaring operations.

Figure 1 Representation of the (a) versatile range of components that can be formed using rotary forming using a simple set of (b) conical top tool and (c) hollow bottom tool

The complex tool path and the localised deformation, although advantageous when it works, poses a big challenge in understanding the mechanics and modelling of the process [(Olga I. Bylya et al. 2018; Krishnamurthy et al. 2017)]. The loading and resulting stress-strain state is non-monotonous, cyclic and significantly triaxial. This in turn renders the design for the processing and shaping of tool kinematics a significant challenge. Previous studies in this area are limited [(Tamang et al. 2017; Montoya et al. 2008; Oudin et al. 1985; Appleton and Slater 1973)] and stock commercial finite element software packages are not well suited to model this process, due in large part to the big uncertainty in having an appropriate material model and assumptions on boundary conditions.

This problem comes to the fore when trying to shape the process for forming near-net shape components. Tubes with flanges of specific angles are a common requirement in the aerospace and automobile industry and are seen as viable components to be produced by rotary forming. With the optimal forming program, it is possible to form these flanges in a single step without any intermediate processing or heat treatment. However, with no established industrial practise, even establishing the first framework for shaping the process is non-trivial. Choosing an appropriate starting material condition, tool kinematic parameters and tool path are complex problems which are impractical to solve by a trial and error method. This is due not only to the fact that the number of parameters are quite large for a design-of-experiments approach, but the parameters are inter-dependant with no readily obvious relations with each other. This results in many process instabilities and failures which are hard to predict and plan against (as shown in Figure 2), and some of these failures can be expensive as they have the potential to not only damage the workpiece but the tools as well as the machine.

Herein, the focus is on a single-step rotary forming of a 90° flange onto hollow tubular components and understanding the instability termed 'internal buckling' observed therein. As shown in Figure 2(a), the need is to form a 90° flange onto an initially straight tube with minimal defects or deviation along the fold. However, in reality, a notable internal flow of material can occur along the inner edge of the fold as shown in Figure 2(b) and 2 (c). Three aerospace materials, namely JETHETE M152 steel, nickel-chromium-cobalt alloy C263 and INCONEL718 have been tested with varying parameters of tube thickness, upstand height, forming method and forming depth. The internal buckling was observed under all conditions to varying degrees. This paper outlines the authors' attempts to quantify the instability, identify the instance of its occurrence, and develop process models to predict it.

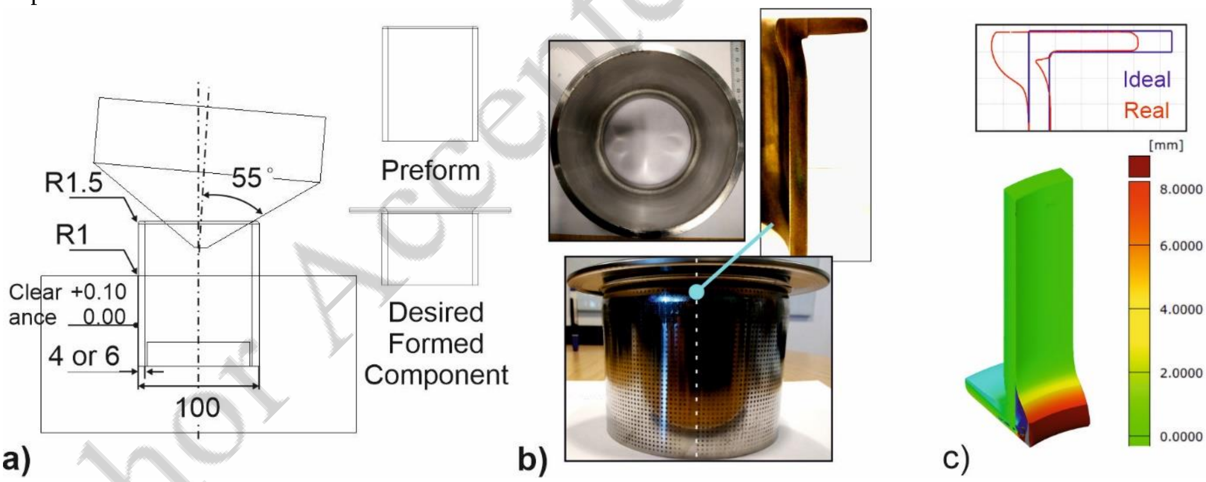

Figure 2 Representation of the (a) preform geometry and desired formed component (b-c) and the internal buckling issue studied. (b) Actual formed component, with the slice used for further study; (c) Comparison of the formed component with ideal expected geometry using proprietary GOM Inspect software

2. Methodology

2.1. Geometry

All preforms used for the trials were of outer diameter 100 mm and length 110 mm. Two different tube thicknesses of 6 and 4 mm were used. Fillets of 1.5mm radius were machined on both edges at the top end (forming end) of the workpiece to ensure smooth initial contact with the top tool. A 55° ($\boldsymbol{\beta}$) top tool was used as it affords possibility for nutation of 35° to the horizontal datum and thereby high flexibility without compromising on the strength of the tool (Tamang et al. 2017). A hollow bottom tool with a cylindrical cavity of a depth of 75 mm, maximum clearance of 0.1 mm with the O.D. of the workpiece and a fillet of 1 mm radius along the top edge was machined to hold the workpiece as shown in Figure 2(a).

2.2. Machine

The Advanced Forming Research Centre of the University of Strathclyde, Scotland is one of the High Value Manufacturing Catapult (HVMC) centres established to bring together academic research and industrial expertise to drive innovation in the UK. In line with this, state-of-the-art rotary incremental bulk forming machines have been installed specifically for industrial-scale research. The MJC RFN 200T-4 machine is one such custom-designed spin-nutation type rotary forging machine. As opposed to the more common orbital type of rotary forging/forming machine, the spin-nutation-type design enables nutation angles ($\boldsymbol{\theta}$) in the range 0° – 45°, with the ability to change it at any time during the process and also apply a maximum load of 200 T at any point in this range. This is especially suited for forming flanges of different angles onto hollow tubes.

The machine has 4 DoF – the top tool can translate vertically, rotate about its own axis and also rotate along the axis perpendicular to the horizontal (termed 'nutation'); while the bottom tool can rotate about its own axis translating this rotation in turn to the workpiece. In order to maintain a rolling contact, the top tool is rotated at a higher velocity ($\boldsymbol{\omega_2}$) proportional to the rotational velocity of bottom tool ($\boldsymbol{\omega_1}$), half-angle of the cone ($\boldsymbol{\beta}$) and the nutation angle ($\boldsymbol{\theta}$) as shown in Figure 3(c) below.

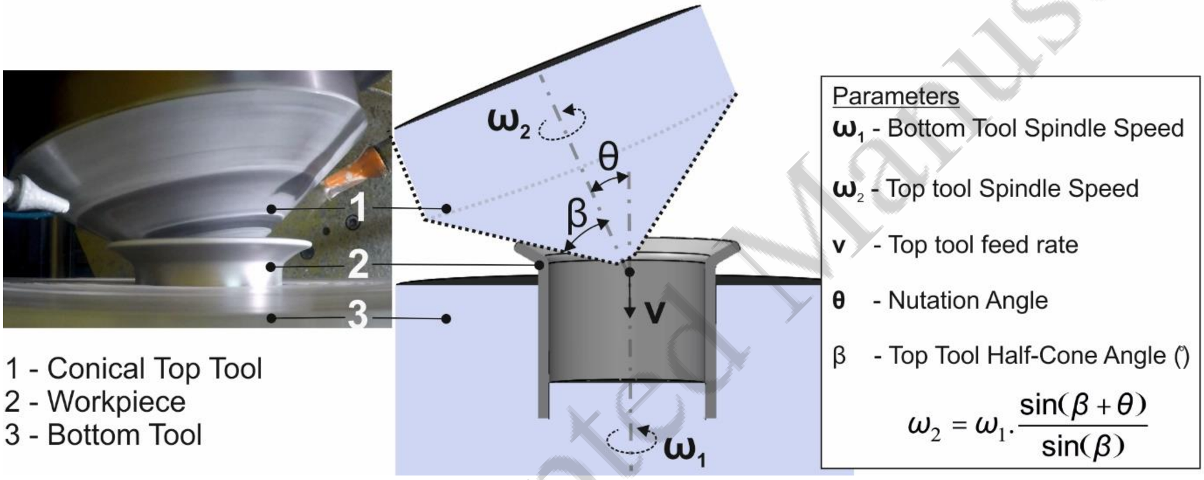

Figure 3 Schematic representation of the rotary forming process with the key kinematic parameters highlighted

2.3. Kinematics

The required rotation speed of the bottom tool, the Z position, X position (which gets translated to the nutation angle), rotation speed and feed rate of the top tool were input in the form of CNC codes to the MJC RFN 200T-4 machine. These values were chosen based on know-how and the fact that they have yielded successful results in the past.

2.4. Forming Method

One of the key aspects that needs to be decided as part of the process design is the forming method to be used. As previously mentioned, owing to the flexibility afforded by the machine, the flanges can be formed in different ways using different top tool paths. Two of the preferred methods are summarised in Figure 4 below. In Method 1, during Stage I (flaring stage), the top tool is allowed to translate towards the workpiece with a small nutation angle to a depth of 14 mm. Following this in Stage II, the top tool is nutated from that depth without any change in the Z position of the top tool. Method 2 differs from 1 in that the top tool is made to translate to a larger depth in Stage I, and then prescribed a simultaneous nutation and vertical translation to achieve the final shape in Stage II as shown in Figure 4.

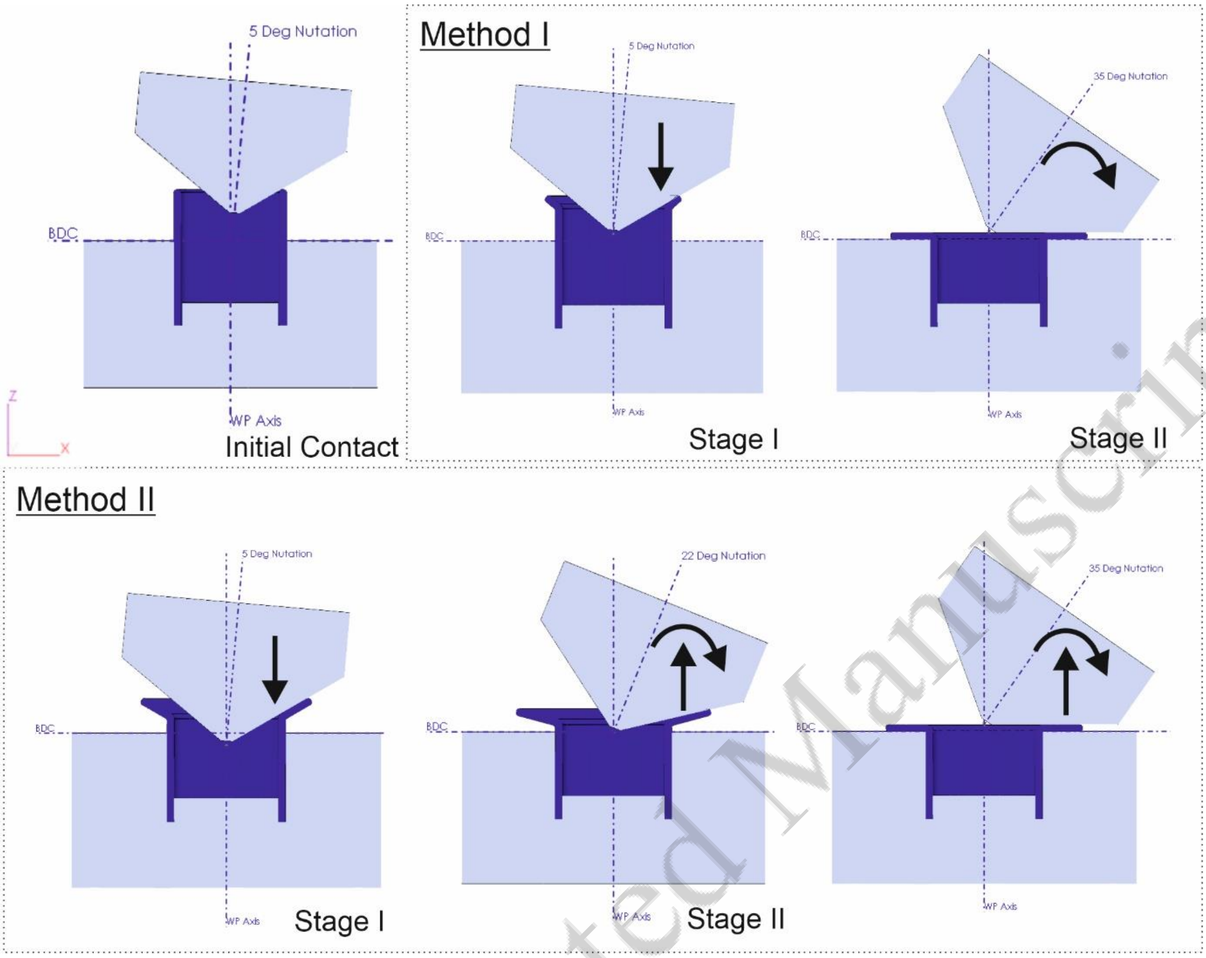

Figure 4 Schematic representation of the different forming routes adopted. Method I involves only nutation in the second stage, while Method II involves both nutation and upwards translation

2.5. Process Modelling and Validation

Finite-element process models were developed in the commercial metal-forming software, QForm, for the project. The kinematic parameters used in the trials were input to the software, and standard friction and heat transfer parameters available in the software database were used in the setup of the model. The problem was formulated as a 3D elasto-plastic one owing to the localized complex cyclic and incremental loading observed in the process. An isotropic hardening material model was used for the three materials, which were developed using the RT tensile data shown in Figure 5. Experimental observation of the temperatures in the component did not exceed the range 100–150°C. It has been reported that the mechanical properties of steels and nickel alloys tended to be nearly strain-rate insensitive at such low temperatures (Dieter 1988; Special Metals 2007) and this was further verified in separate tensile tests. Hence, RT material data was deemed to be representative enough. The detailed modelling methodology used and the challenges faced in modelling rotary forming processes are summarised in earlier works [(Krishnamurthy et al. 2017; Tamang et al. 2017; Bylya et al. 2017)].

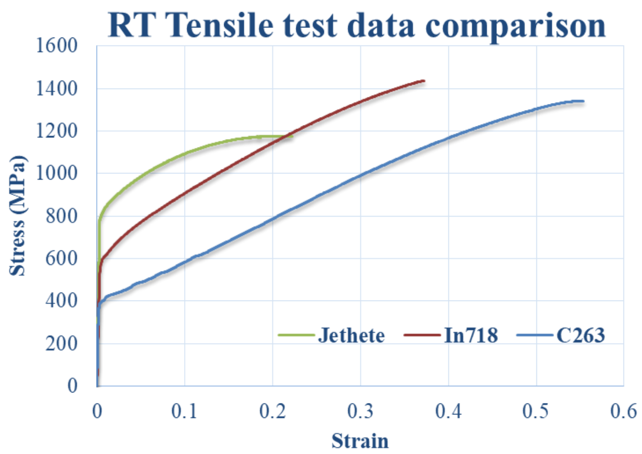

Properties	Jethete	IN718	C263
Young's Modulus, E (GPa)	216	189	220
Yield Stress, σ_y (MPa)	787	574	404
Ultimate tensile, stress, σ_u (MPa)	1175	1437	1341
Normalised strain hardening/softening factor, γ	0.12	0.30	0.44
Limiting tensile elongation, δ	0.22	0.37	0.55

Figure 5 Summary of room temperature tensile test data for the three materials studied

To validate the model, the load, geometry, strain and temperature data obtained from the experiments were used. The calibration procedure is summarised in Figure 6 below, wherein the geometry and temperature profile generated through the trials, as observed from a high-definition video and thermal image capture, respectively, were used to validate the values obtained in the process models. Similarly, the forming load traces recorded on the machine were used for validating those obtained from the process models. The output geometry obtained from the full and interrupted trials were measured as well as scanned for analysis. To get a clear image of the region of folding, thin slices of width 20 mm were cut (as shown in Figure 2(b)) from the tubes and then photographed. These were then processed and compared with those obtained from the process models (exported as .STL files) in proprietary GOM Inspect software (Figure 6(c)).

In addition, an electrochemically etched rectangular dot grid system, commonly used in sheet metal forming limit identification, was used to determine the strain on the deformed surface of the tubes here. These were then used for validating the strain profile observed in the FE simulation (Figure 6(d)).

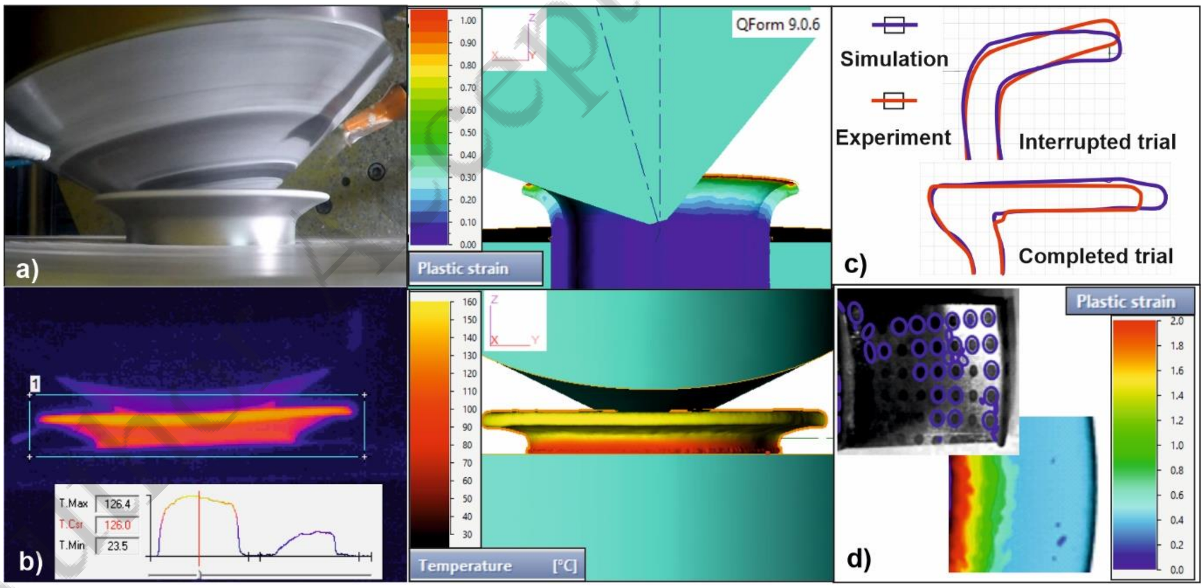

Figure 6 Validation methodology used for the process models – validation with through-process recording (a) metal flow with the high-definition video and (b) temperature profile with that of the thermal camera recording; and validation of (c) output geometry by GOM comparison and (d) strain profile using the image processing method

3. Results and Discussion

3.1. Identification and Quantification of Instability

To identify the origin of the instability, interrupted trials were planned, i.e. the trials were stopped at the instance of starting of the instability. To determine this point, videos obtained for preliminary trials from the high-definition cameras were processed using a commercial video processing software. The videos were trimmed to the exact duration of the process, following which linear guidelines were used to identify the exact instance of the commencement of instability, as shown in Figure 7 below. This was then compared with the machine data and process simulation to translate this point in time to the nutation position of the top tool. As can be observed in Figure 7, the onset of instability is early in the nickel alloys (at 22° nutation in stage II), while it happens at a later stage in Jethete (at 26° nutation in stage II). Interrupted trials were carried out for the materials where the process was stopped at the points identified.

The interesting aspect to be noted here is the profile formed by Jethete and C263 at the onset of instability. This profile could also be observed in the completely formed geometry as well, as can be derived from Table 2, and gives clues to understanding the prevalent buckling in Nickel alloys compared to that in Jethete. More study on this aspect is needed to understand completely the origin of such a buckling effect and how to avoid it for new materials.

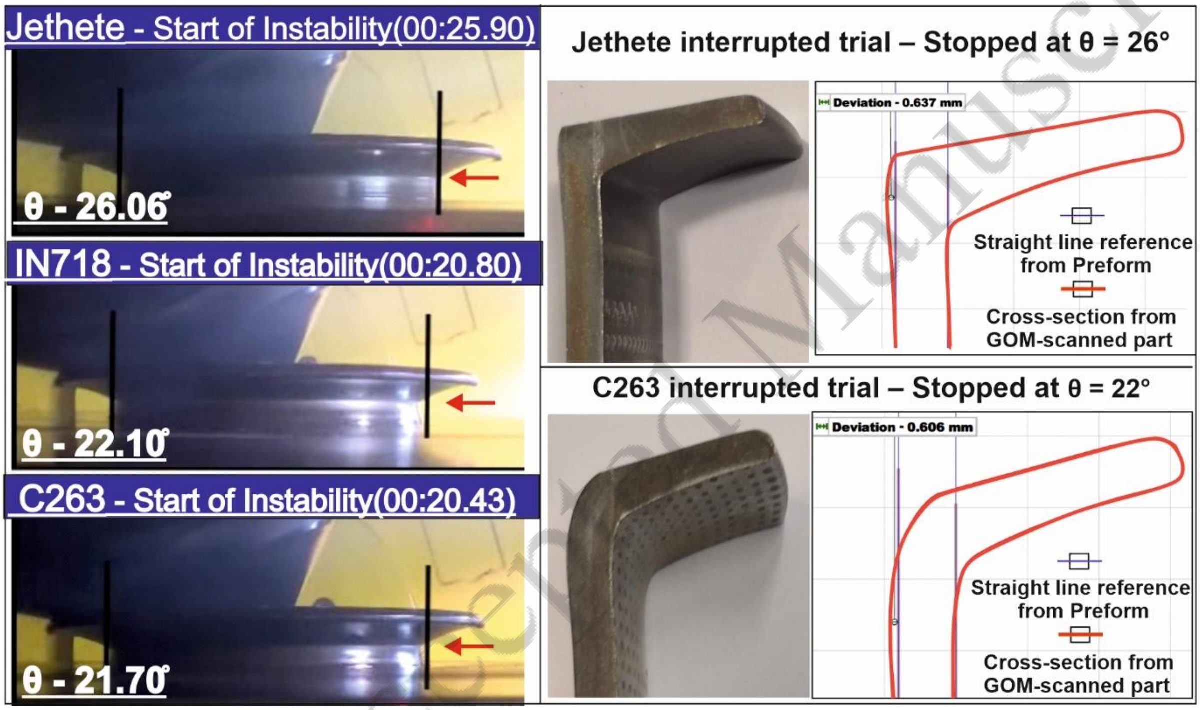

Figure 7 Representation of the high-definition video capture analysis carried out to identify the instances of instability in the three different materials

To quantify the instability, the key features of the formed component, outer diameter and inner diameter of the flange and the thickness at the outer and inner part of the flange, were measured using a Vernier Calliper. Three measurements were taken each time and the average of the three measurements were used for analysis. The hoop strain values were then calculated with respect to the initial circumference. These are summarised in Table 2 below. In addition, thin slices of 20 mm width were also cut from the specimens and analysed with respect to the ideal expected geometry as shown in Figure 2(c).

Table 2 Comparison of the output geometries for difference material and thickness

Thickness	Part No.	I.D.	Int. hoop strain	O.D.	Ext. Hoop Strain
Jethete					
6	223-5	82.49	**(-)0.06**	141.89	**0.42**
4	232-5	80.30	**(-)0.13**	140.92	**0.41**
C263					
6	223-12	80.6	**(-)0.08**	141.2	**0.41**
4	232-3	77.54	**(-)0.16**	134.63	**0.35**
IN718					
6	223-17	78.6	**(-)0.11**	139.7	**0.40**
4	232-1	75.8	**(-)0.18**	133.08	**0.33**

3.2. Fine-tuning of Process models

Validation and prediction of the output geometry was one of the most challenging aspects of developing a more robust model for the rotary forming process. More specifically, the ability to capture the buckling effect observed in the forming trials is non-trivial and required a few unconventional techniques. Using the conventional method of modelling such a finite deformation process – specifically, a strain-based remeshing technique – material flow behaviour near the fold in the flange could not be captured in the process model. Modification of the hardening behaviour in the material models did not yield positive results and the process model was still unable to capture the internal flow of material during the nutation stage. The use of a standard tetrahedral solid element mesh and remeshing technique was later identified to be the reason for this effect. Through remeshing, wherein the Finite-Element (FE) software continuously tries to realign and change the local mesh elements in the areas of high deformation, somehow rendered the material "soft" and flow in an ideal way to help in the convergence of results.

The prevalent buckling effect observed in the trials carried out with the thinner (4 mm) tubes was very helpful in fine tuning the process model. Figure 8 below provides a summary of the stages in the fine-tuning of the model. As a first step, a brick (rectangular) shell mesh element was used without remeshing criteria. This seemed to yield better geometry prediction and was able to predict the output geometry with the buckling effect. In addition, it was also possible to capture the difference in the flow behaviour around the fold between Jethete and C263, as seen in Figure 8. In addition, using the brick mesh without remeshing, it was possible to bring down the simulation time considerably, from 3 weeks to 3 days.

However, this method was still prone to some inaccuracy in geometry prediction, as was observed when validating the process model with interrupted trials. While the process model was able to predict the final output geometry, it still predicted the metal flow in intermediate stages of forming with error as shown in Figure 8.

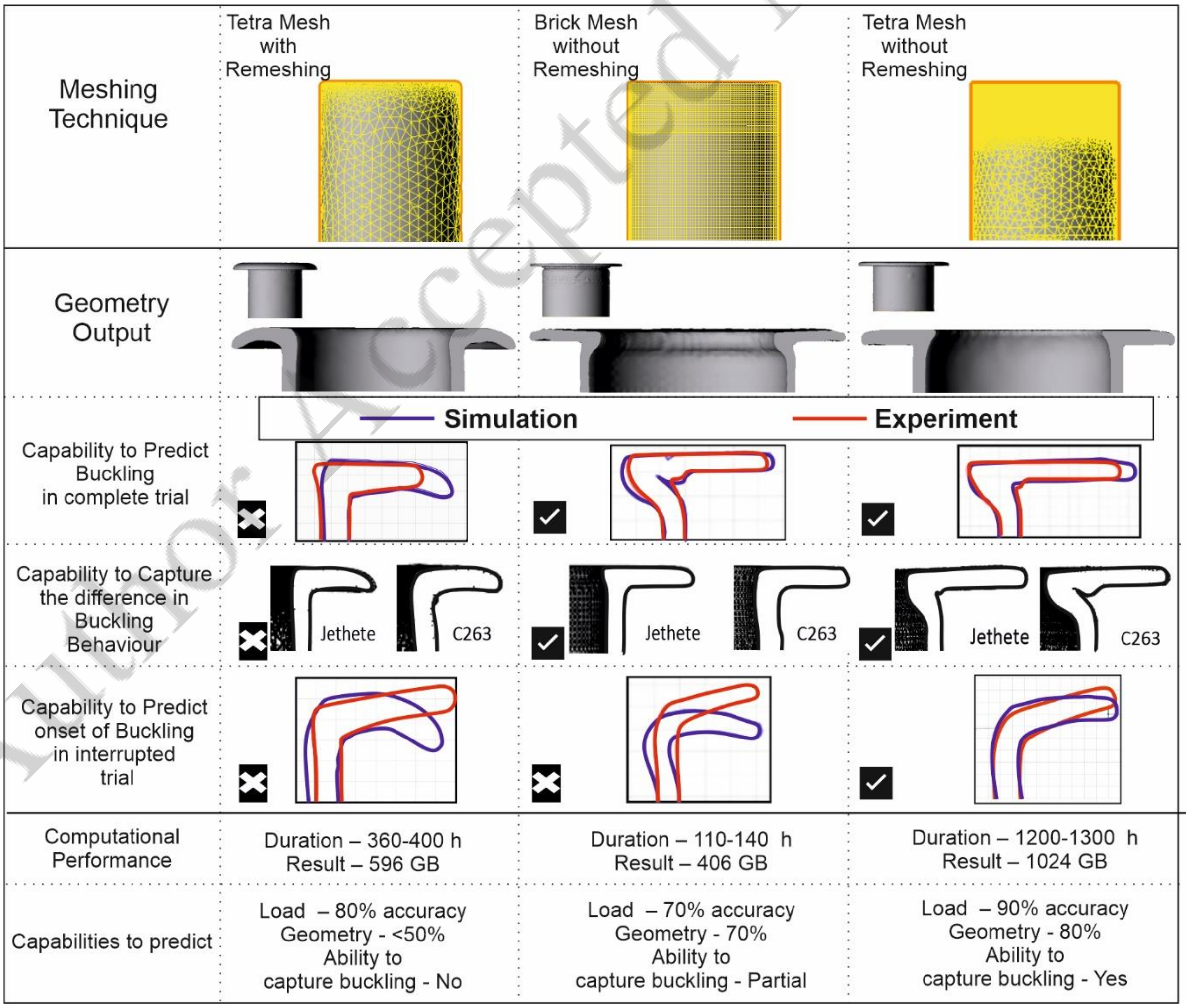

Figure 8 Representation of the increase in maturity of geometry prediction in the process models (a) preliminary stage (b) intermediate stage using a brick mesh without remeshing, (c) improved state using a tetra mesh without remeshing

The use of a solid tetrahedral mesh, without remeshing, however, seemed to improve the geometry prediction in intermediate stages as well, and was found to provide better representation of the material flow. The use of this method did seem to increase the simulation time compared to that of the brick mesh. Therefore, the suggestion would be to run initial simulations with a brick mesh without remeshing for preliminary iterations to test hypotheses, while a solid tetra mesh without remeshing is recommended for final simulations. The lack of remeshing seemed to cause some problems while simulating Method 2 type of forming, as the tool path tends to produce a highly distorted mesh in stage II. In such a case, it was found to be useful to stop the simulation at the start of mesh distortion, remesh the local region for a short while and then continue the simulation without remeshing until further inacceptable distortion of the mesh.

3.3. Preliminary Improvements through Process Models

The validated process model was used to glean some insight into the mechanics of rotary flange forming and devise some recommendations to eliminate or at least reduce the internal buckling. As shown in Figure 9 below, the load trace and geometry development were analysed using the process model. The load trace in conjunction with the geometry observed in the process model provided some hints to the start of internal buckling. It is hypothesised that at the trough of the load trace the forming mechanism changes. This critical point, termed as the 'inflection point' herein, is shown for the three materials and two different thicknesses in Figure 9(a). This was used in the shaping of our process (as shown in Figure 9(b)), but further in-depth study on the process mechanics will be useful to translate the results to new materials and geometry.

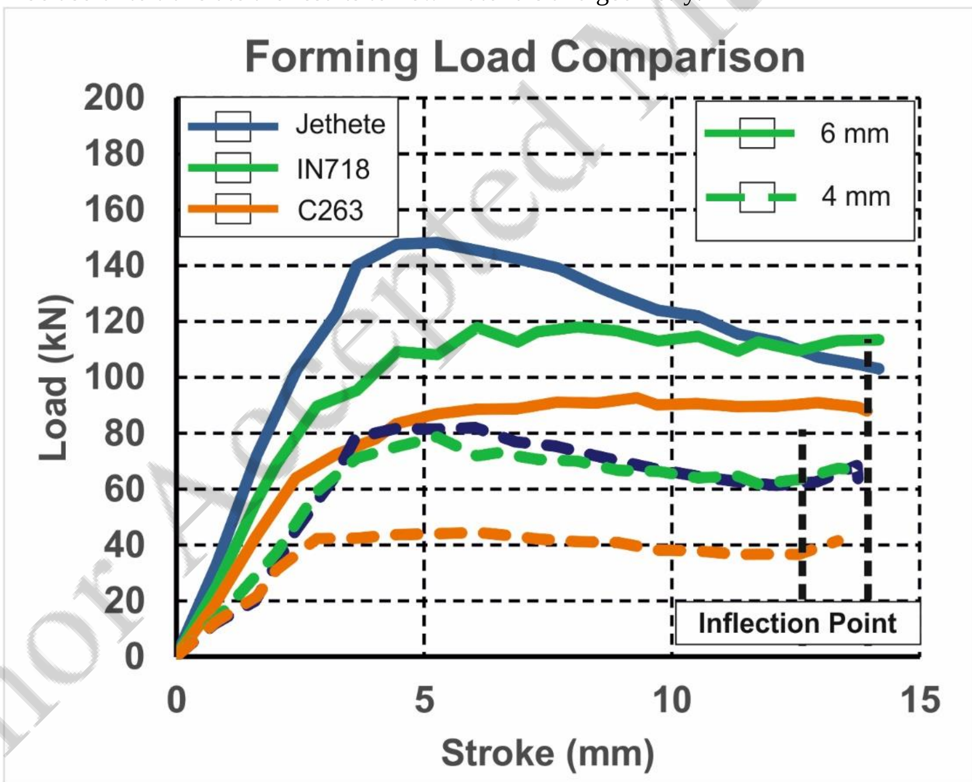

(a)

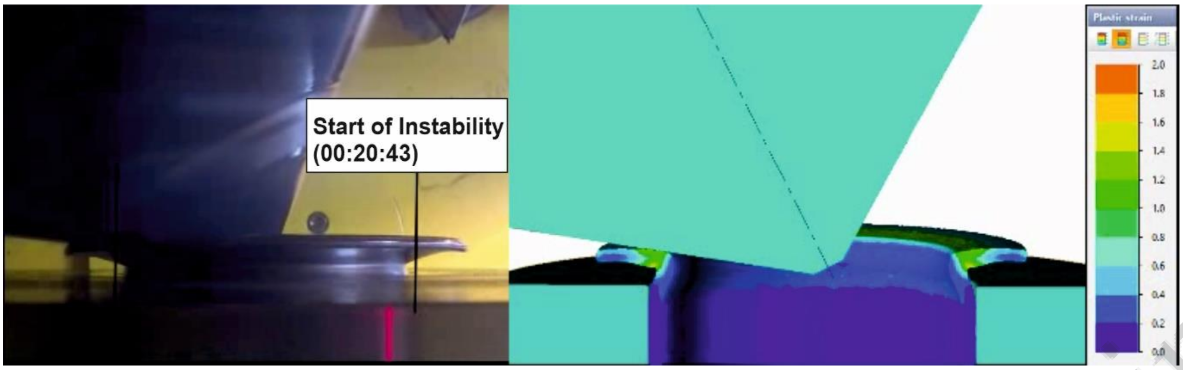

(b)

Figure 9 Preliminary results from the improved process model (b) comparison of the forming load trace for Jethete, IN718 and C263, (c) Prediction of the start of instability using the process model

The geometry prediction capability of the process model (as shown in Figure 9(b)) were used to shape the process and compare the results for the different forming methods. Table 3 shown below, compares the output geometry obtained using the improved process using Method 2 with that of the initial process using Method 1. As can be seen from the measurements and GOM scan analysis shown in Table 3, the use of Method 2 seems to result in reduced buckling than that observed with Method 1. Only Jethete and C263 were tested in this case, as a representative for steel and nickel alloy. In both cases, there were pronounced improvements in the output geometry. The combination of Z motion and nutation of the top tool seemed to prevent the drastic internal movement of the workpiece. Although the thickness distribution in the formed component seemed to be non-uniform in the case of Method 2, it did result in a better forming along the inner edge (part in contact with the bottom tool) of the flange. The lack of fold along the inner edge was a positive sign and the component could easily be subjected to a further machining operation to achieve the end result.

Table 3 Comparison of the output geometries for trials carried out using Method 1 and 2

Material	Measure	Method 1	Method 2	GOM Section Comparison
Jethete	I.D.	78.91	86.46	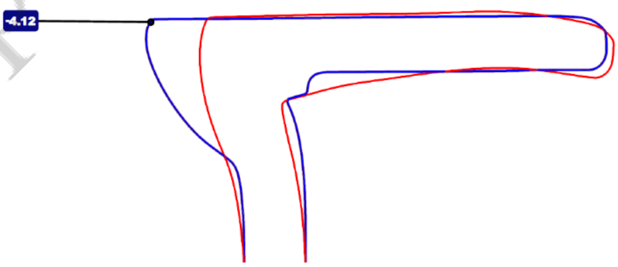 Comparison – Method 1 (Blue) and 2 (Red)
	O.D.	139.95	141.48	
C263	I.D.	77.45	81.96	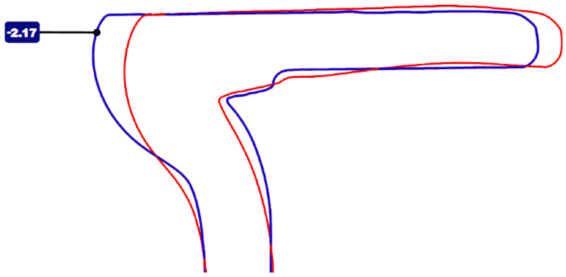 Comparison – Method 1 (Blue) and 2 (Red)
	O.D.	134.73	138.31	

Conclusions

Herein, a systematic analysis of internal buckling observed in rotary forming of a 90° flange using different aerospace-grade alloys with different tube thicknesses were carried out. Methods for quantifying the instability and identifying the instances of its occurrence were identified and novel validation methodology was developed to fine-tune an FE model for the process, which were lacking hereinbefore. The main contribution from the present work were the use of validated process models to gain some basic understanding of the mechanics of rotary forming and to assist in the shaping of the rotary forming process to yield improved results.

The use of a combined nutation-translation type top tool motion (Method 2) during the flange forming stage was found to result in reduced buckling than that observed with only nutation (Method 1) for both Jethete and C263. This can be used to inform forming strategies for the future. Furthermore, buckling was observed to be more prevalent, to happen earlier, and to occur in a different way in nickel alloys than in Jethete steel. The aspects of the material properties that leads to this effect need to be studied further to help effect successful trials using material preparation techniques such as heat treatment.

Acknowledgement

The authors would like to acknowledge Rolls Royce Plc for funding this work from their Innovate UK: Aerospace Technology Institute Strategic R&D Project grant (application no. 66733-263147) titled "Manufacturing Portfolio Project 2: Manufacture of Advanced Materials". We would also like to thank the AFRC's Forging and Incremental Processes team for their excellent support, guidance and provision of resources throughout the project. Most importantly, we greatly appreciate the time spent by key staff in both Rolls-Royce and AFRC in support of this project.

References

Appleton, E., and R. A.C. Slater. 1973. "Effects of Upper Platen Configuration in the Rotary Forging Process and Rotary Forging into a Contoured Lower Platen." *International Journal of Machine Tool Design and Research* 13 (1): 43–62. https://doi.org/10.1016/0020-7357(73)90030-9.

Bylya, O. I., M. Ward, B. Krishnamurty, S. Tamang, and R. A. Vasin. 2017. "Modelling Challenges for Incremental Bulk Processes despite Advances in Simulation Technology: Example Issues and Approaches." *Procedia Engineering* 207 (September): 2358–63. https://doi.org/10.1016/j.proeng.2017.10.1008.

Bylya, Olga I., Timur Khismatullin, Paul Blackwell, and Rudolf A. Vasin. 2018. "The Effect of Elasto-Plastic Properties of Materials on Their Formability by Flow Forming." *Journal of Materials Processing Technology* 252 (September 2017): 34–44. https://doi.org/10.1016/j.jmatprotec.2017.09.007.

Dieter, G. E. 1988. "Mechanical Metallurgy. 3rd Ed." In *Mechanical Metallurgy*, 3rd revise, 23:194–194. London: McGraw-Hill Book Company (UK) Limited. https://doi.org/10.1002/crat.2170230211.

Groche, P., D. Fritsche, E. A. Tekkaya, J. M. Allwood, G. Hirt, and R. Neugebauer. 2007. "Incremental Bulk Metal Forming." *CIRP Annals - Manufacturing Technology* 56 (2): 635–56. https://doi.org/10.1016/j.cirp.2007.10.006.

Krishnamurthy, Bhaskaran, Olga Bylya, Lisa Muir, Alastair Conway, and Paul Blackwell. 2017. "On the Specifics of Modelling of Rotary Forging Processes." *Computer Methods in Materials Science* 17 (1): 22–29.

Montoya, I., M. T. Santos, I. Pérez, B. González, and J. F. Puigjaner. 2008. "Kinematic and Sensitivity Analysis of Rotary Forging Process by Means of a Simulation Model." *International Journal of Material Forming* 1 (SUPPL. 1): 383–86. https://doi.org/10.1007/s12289-008-0075-3.

Oudin, J., Y. Ravalard, G. Verwaerde, and J. C. Gelin. 1985. "Force, Torque and Plastic Flow Analysis in Rotary Upsetting of Ring Shaped Billets." *International Journal of Mechanical Sciences* 27 (11–12): 761–80. https://doi.org/10.1016/0020-7403(85)90008-6.

Special Metals. 2007. "IN718 Datasheet," 1–28. https://doi.org/SMC-066.

Tamang, Subha, Olga Bylya, Michael Ward, Xichun Luo, Steven Halliday, and Martin Tuffs. 2017. "Comparison between Rotary and Conventional Flaring Processes." *AIP Conference Proceedings* 1896: 1–8. https://doi.org/10.1063/1.5008047.